NACA RM No. L8A28c

NACA

RESEARCH MEMORANDUM

EFFECTS OF SWEEP ON CONTROLS

By

John G. Lowry, John A. Axelson, and Harold I. Johnson

Langley Memorial Aeronautical Laboratory
Langley Field, Va.

NATIONAL ADVISORY COMMITTEE
FOR AERONAUTICS

WASHINGTON

June 3, 1948

Declassified February 10, 1956

NACA RM No. L8A28c

NATIONAL ADVISORY COMMITTEE FOR AERONAUTICS

RESEARCH MEMORANDUM

EFFECTS OF SWEEP ON CONTROLS

By John G. Lowry, John A. Axelson, and Harold I. Johnson

SUMMARY

An analysis of principal results of recent control-surface research pertinent to transonic flight has been made. Available experimental data on control surfaces of both unswept and sweptback configurations at transonic speeds are used to indicate the control-surface characteristics in the transonic speed range. A design procedure for controls on sweptback wings based on low-speed experimental data is also discussed.

The results indicated that no serious problems resulting from compressibility effects would be encountered as long as the speeds are kept below the critical speed of the wing and the trailing-edge angle is kept small. Above critical speed, however, the behavior of the controls depended to a large extent on the wing sweep angle.

The design procedures presented for controls on swept wings, although of a preliminary nature, appear to offer a method of estimating the effectiveness of flap-type controls on swept wings of normal aspect ratio and taper ratio.

INTRODUCTION

The design of controls for unswept wings that fly at low speed has been discussed in several papers (references 1 to 7). The design procedures set forth in these papers are adequate to allow for the prediction of control characteristics within small limits. However, with airplane speeds approaching and sometimes exceeding the critical speed of the wing surface, these low-speed characteristics are drastically changed. This paper will use the results of about 25 investigations (references 8 to 26) to indicate the nature of these changes and to discuss the design of controls on swept wing.

At the present time, information on the behavior of controls in the transonic-speed range is too meager to permit the development of a rational design procedure that applies at transonic speeds. Because of this situation, the design of control surfaces for transonic airplanes must still be based primarily on low-speed considerations. At the same time, however, the experimental results that are available for transonic speeds indicate certain trends which should be kept in mind in order to reduce the unfavorable effects of compressibility at high speeds. With this thought in mind, therefore, some of the important experimental data at transonic speeds will be discussed and a design procedure based on low-speed data will be presented. For convenience, the discussion will be divided into aileron effectiveness, lift effectiveness, pitching-moment effectiveness, and hinge-moment characteristics. However, it should be realized that the parameters are closely interdependent and hence, if a certain geometric design feature causes a particular change in one of the parameters, it will usually cause a corresponding change in the others.

SYMBOLS

C_L	lift coefficient (Lift/qS in which lift is in pounds)
C_l	rolling-moment coefficient (L/qSb)
C_m	pitching-moment coefficient (Pitching-moment/qSc' in which pitching moment is in foot-pounds)
C_h	hinge-moment coefficient $\left(H/qS_f\bar{c}_f\right)$
$\bar{c}_l$	mean control chord normal to hinge line, feet
L	rolling moment, foot-pounds
H	hinge moment about hinge line, foot-pounds
S	wing area, square feet
S_f	area of control surface, feet
b	wing span, feet
c	local chord, feet
c'	mean aerodynamic chord, feet
$\bar{c}_f$	control chord normal to hinge line, feet
t	airfoil thickness, feet

q dynamic pressure of free stream

M Mach number

R Reynolds number

δ control deflection about hinge line, degrees

α_δ effective change in wing angle of attack caused by unit angular change in control-surface deflection

Λ sweep of wing leading edge, degrees

$$C_{L_\delta} = \left(\frac{\partial C_L}{\partial \delta}\right)_\alpha$$

$$C_{l_\delta} = \left(\frac{\partial C_l}{\partial \delta}\right)_\alpha$$

$$C_{m_\delta} = \left(\frac{\partial C_m}{\partial \delta}\right)_\alpha$$

$$C_{h_\alpha} = \left(\frac{\partial C_h}{\alpha}\right)_{\delta=0}$$

$$C_{h_\delta} = \left(\frac{\partial C_h}{\delta}\right)_{\alpha=0}$$

$C_l/\Delta\alpha$ rolling-moment coefficient caused by a unit difference in wing angle of attack of various right and left portions of a complete wing

$\frac{pb}{2V}$ wing-tip helical angle

p rate of roll

V free-stream velocity

Subscripts:

a aileron

t tab

AILERON EFFECTIVENESS

Effects of Compressibility

Effects of sweep.- Information on the effect of sweep on aileron effectiveness at high subsonic speeds was obtained recently from tests in the Langley 8-foot high-speed tunnel (references 8 and 9). These tests were run on a wing of NACA 65-210 section which for the unswept case had an aspect ratio of 9.0, a taper ratio of 0.4, and a 20-percent-chord plain aileron covering 37.5 percent of the wing semispan near the tip. In order to obtain the swept-wing configurations, the straight wing was rotated about the 40-percent-root-chord point and the tips extended so that they were parallel to the air stream. This procedure changed somewhat the aspect ratio, taper ratio, and wing section parallel to the stream direction but retained the advantages inherent in testing the same model at different angles of sweep. Some typical results from the investigation are shown in figure 1.

Here we have the change in rolling-moment coefficient produced by 20° change in total aileron angle plotted against Mach number for the straight wing and for the two wings sweptback 32.6° and 47.6°. It is noted that the ailerons on the straight wing remained fully effective up to the critical Mach number of the wing which was 0.73 at design lift coefficient. Beyond the critical Mach number the ailerons continued to lose effectiveness up to the highest test Mach number of 0.925. This large loss in rolling-moment effectiveness at supercritical Mach numbers is apparently a direct reflection of the generally large loss in lift effectiveness of trailing-edge control surfaces on straight airfoils at supercritical Mach numbers. The effects of sweepback are seen to be twofold. First, the aileron effectiveness, before compressibility effects appear, is reduced approximately by the factor $\cos^2\Lambda$ in accordance with the simple theory of the effect of sweepback on flap effectiveness. Second, the Mach number at which compressibility effects first appear is raised by sweeping the wing back. For example, the aileron on the straight wing began to lose effectiveness at a Mach number of about 0.7, that on the 32.6° sweptback wing at a Mach number of 0.8, and that on the 47.6° sweptback wing at a Mach number of 0.9. It might be noted also that the drop-off in effectiveness due to compressibility effects becomes less abrupt as the sweepback angle is increased. These data show the desirability of resorting to sweepback in order to delay the loss in aileron control effectiveness that occurs at high subsonic speeds.

Some qualitative data on the effectiveness of ailerons at Mach numbers between the critical and 1.3 have been obtained by the Langley Pilotless Aircraft Research Division (reference 10) and are shown in figure 2. In these tests rocket-propelled test vehicles were fitted

with low-aspect-ratio wing of NACA 65-series section having 20-percent-chord sealed ailerons deflected about 5° parallel to the relative wind. From continuous measurements of the rolling velocity and speed of the missiles the rolling-effectiveness parameter pb/2V was determined as a function of Mach number. It should be noted that this parameter pb/2V depends on the wing damping moment due to rolling as well as the aileron effectiveness so that some of the results are only qualitative with regard to aileron effectiveness. However, the results probably indicate correctly the effects of the various major design parameters on aileron effectiveness at transonic speeds. In figure 2 we have plotted the pb/2V per degree of aileron deflection against the flight Mach number. It is seen that for these wings of 9-percent thickness and aspect ratio of 3 the unswept configuration experiences a sudden serious loss in aileron effectiveness at Mach numbers around 0.925. Because of the effects of rotational inertia of the rocket-propelled body and the longitudinal deceleration during these tests, the actual loss in effectiveness was somewhat greater than is shown by the data. As the sweepback angle is increased, the abrupt loss in effectiveness grows smaller until at a sweepback angle of 45° there appear to be no sudden changes in effectiveness through the transonic range. The aileron effectiveness at supersonic speeds is much less than at subsonic speeds for all sweepback angles, the difference being greatest for the unswept wing and least for the most highly swept wing.

Effect of thickness.- Other rocket tests (reference 10) have shown that airfoil section thickness appears to have a major effect on the loss in effectiveness of controls in the transonic range. Figure 3 illustrates this point. Here we have tests of two NACA 65-series symmetrical airfoils of different thickness ratios at an aspect ratio of 3.0. The 9-percent-thick section exhibited an abrupt loss in effectiveness at a Mach number of 0.925, but the 6-percent-thick section, although showing an equal loss in effectiveness from Mach number of 0.9 to 1.3, does not show the discontinuity at Mach numbers of about 0.9. Data for sweptback wings similar to that shown here indicated that for 45° sweepback, sudden changes in control effectiveness in the transonic-speed range will be avoided if the thickness ratio is less than 10 or 12 percent. These data apply for deflections of 5° and therefore may not represent the variations for smaller deflections.

Effect of aspect ratio.- The effect of aspect ratio at 45° sweepback as determined from rocket tests (reference 10) is shown in figure 4. The control on the airfoil of aspect ratio 1.75 was considerably more effective than that of the airfoil of aspect ratio 3.0. This may very well be largely an effect of change in the damping moment due to rolling of the airfoils. The same trend in control effectiveness with aspect ratio was observed also on unswept airfoils of aspect ratio 1.75 and 3.0.

Effect of trailing-edge angle.- The trailing-edge angle of controls also appears to determine to a large extent the behavior of ailerons at

transonic speeds. Some results from the Langley 8-foot high-speed tunnel (reference 8) and from the Ames 16-foot high-speed tunnel are shown in figure 5. This figure shows the rolling moment produced by aileron deflection for several wings at 2° angle of attack and at Mach numbers of about 0.85. We see that the aileron with a 20° trailing-edge angle on the unswept 12-percent-thick wing showed a reversal in effectiveness for the up-going aileron. This reversal of effectiveness extended to deflections of 10°, the largest tested. The aileron with the 11° trailing-edge angle on the unswept 10-percent-thick wing did not however show any reversal even at slightly higher Mach numbers. Sweeping the wing with the large trailing-edge angle back 47°, as shown in this figure, also eliminated the reversal in effectiveness over the complete deflection range. Other Ames 16-foot high-speed-tunnel data (reference 14) indicate, however, that the trailing-edge angle of controls on swept wings is also critical. For example, ailerons with 16.4° trailing-edge angle on a 37° sweptback wing showed serious decreases in effectiveness with Mach number, whereas reducing the trailing edge to 11.2° alleviated the large decrease in effectiveness. These results indicate two things: first, that the trailing-edge angle is important and should be kept as small as possible, and second, that sweeping the wing will reduce but will not necessarily eliminate the adverse effects of large trailing-edge angles on aileron effectiveness.

Aileron Design

Experimental results.- From the discussion thus far we see that the main effects of sweep are to delay the adverse effects of compressibility to higher Mach numbers and to reduce the magnitude of these effects when, and if, they do occur. In order to determine to what extent the design procedure for controls on unswept wings would have to be modified for swept wings, a semispan wing with an aspect ratio of 6 and taper ratio of 1/2 was tested in the Langley 300 MPH 7- by 10-foot tunnel, unswept and with three sweep angles. The wing was equipped with a variable-span, plain-sealed, 20-percent-chord aileron.

The variation of the rate of change of rolling-moment coefficient with deflection C_{l_δ} with span of aileron for the various angles of sweep is shown in figure 6. The aileron for this investigation extended inboard from the tip but the data are applicable for other aileron locations. The variation of C_{l_δ} with sweep shown here also includes the effect of aspect ratio which varied from 6 for the straight wing to 3.43 for the 51.3° swept wing. It will be noted that as the sweep is increased and the aspect ratio decreases, the values of C_{l_δ} decrease considerably and that this decrease is even greater for ailerons located near the wing tip. It should be remembered, however, that these data

are for low Mach numbers and Reynolds number of about 2×10^6. In order to make this chart of a more general nature, the data were reduced to the form more generally used - that is, the change in rolling moment for unit change in angle of attack over the aileron span $C_l/\Delta\alpha$. In making this reduction it was necessary to establish a nomenclature for swept wings. In order to be consistent with established procedures, the chords and spans of the swept wings are measured parallel and perpendicular to the plane of symmetry and the sweep angle is that of the wing leading edge. (See fig. 7.) The control-surface deflections are measured in a plane perpendicular to the control hinge line. When the "unswept" wing panel is referred to, it will represent the wing that would be obtained if the swept wing were rotated about the midpoint of the root chord until the 50-percent-chord line is perpendicular to the plane of symmetry. The tip is cut off parallel to the plane of symmetry. The chords in this case are measured perpendicular to the 50-percent-chord line. (The unswept spans and chords are primed in fig. 7.)

Design procedure.- In reducing the data of figure 6 from C_{l_δ} to $C_l/\Delta\alpha$ as shown in figure 8, the values of C_{l_δ} at each spanwise station were divided by $\cos^2\Lambda$ and the value of flap effectiveness parameter α_δ for the "unswept" wing panel. This method resulted in obtaining an average curve for large-span ailerons and ailerons on wings swept less than 40° that agreed with the theoretical curve (reference 2) for the same aspect ratio and taper ratio as the unswept wing. Short-span tip ailerons show, however, a loss in effectiveness for the higher sweep angles and indicate that on highly swept wings a partial-span aileron located slightly inboard will give more rolling moment than the same aileron located at the wing tip.

In using this chart for design purposes, it is necessary to correct the values of $C_l/\Delta\alpha$ for aspect ratio, taper, and flap chord. Aileron effectiveness C_{l_δ} is obtained by using the formula at the top of the figure where $C_l/\Delta\alpha$ is obtained from the appropriate curve on this chart. The aspect-ratio correction K_1 is the ratio of $C_l/\Delta\alpha$ for the aspect ratio of the "unswept" wing to the value of $C_l/\Delta\alpha$ for aspect ratio 6 (obtained from reference 2) and for taper ratio of 1/2. The taper-ratio correction K_2 is the ratio of the value of $C_l/\Delta\alpha$ for the taper ratio of the "unswept" wing to the value of $C_l/\Delta\alpha$ for taper ratio of 1/2; both values (obtained from reference 2) are for aspect ratio 6. The flap-effectiveness parameter α_δ is based on the unswept-aileron-chord ratio (see reference 1) and Λ is the sweep of the wing leading edge. The values of C_{l_δ} thus obtained are for low

lift coefficients and for small deflections, and some changes will occur if either is varied considerably.

Effect of deflection.- Figure 9 shows the ratio of C_{l_δ} obtained at large aileron deflections to the values of C_{l_δ} obtained from the previous figures. It will be noted that the loss in C_{l_δ} for larger deflections is less for the swept wing than for the straight wing. The difference appears to be about the same as the difference in deflections of the ailerons on the two wings measured in the stream direction. Thus, it would appear that larger deflections can be used on swept wings which would tend to alleviate the low effectiveness of the ailerons. The results of swept-wing-aileron investigations indicate that the effectiveness, as with straight wings, is relatively constant with lift coefficient so long as no unusual or sudden changes in flow occur over the wing.

Comparison of estimated and test results.- In order to determine the reliability of this method in predicting C_{l_δ} for wings of other sweeps, aspect ratios, and taper ratios, values of C_{l_δ} were estimated for 14 wings and are compared in figure 10 with the measured values.

Figure 10 is a plot of $C_{l_{\delta_{est}}}$ against $C_{l_{\delta_{test}}}$; the solid line is the line of agreement. The scatter of points around the line of agreement indicates that the method gives good agreement for these rather conventional sweptback wings, that is, wings of aspect ratio between 2.5 to 6 and taper ratios between 0.4 to 1. This method, however, cannot be expected to give as good results for all cases of swept wings, particularly for those of extremely low aspect ratio and/or with extreme taper.

LIFT EFFECTIVENESS

Effects of Compressibility

Effects of sweep.- The problem of control lift effectiveness is closely related to the problem of aileron rolling effectiveness. In the case of ailerons, we are interested in the rolling moment caused by the lift effectiveness of a control located some distance outboard on a wing. In the case of an elevator or a rudder, we are interested directly in the lift effectiveness of the control, inasmuch as this lift effectiveness determines how much elevator control will be required to pitch the airplane through its angle-of-attack range or how much

rudder control will be required to offset yawing moments due to the use of ailerons, asymmetric power, and so forth. Because of the close functional relationship between all the primary controls, therefore, one might expect to find that the effects of compressibility on the lift effectiveness of elevators and rudders will be largely the same as the effects of compressibility on the rolling-moment effectiveness of ailerons and vice versa. This expectation is borne out by an analysis of the available experimental data pertaining to full-span controls that would likely be used as elevators and rudders. Some effects of compressibility on the lift effectiveness of such controls will be considered now.

An examination of the data for full-span control surfaces on unswept airfoils, tested recently in the Langley 8-foot high-speed tunnel, the Langley 16-foot high-speed tunnel, and the Langley 24-inch high-speed tunnel (references 13 and 22 to 25), permit two conclusions to be made regarding lift effectiveness at high subsonic speeds. First, below the critical speed of the airfoil the control lift effectiveness is essentially unaffected by compressibility effects. Second, at speeds slightly above the critical speed the controls tested always experienced an abrupt loss in effectiveness which continued up to the highest speed tested. The data suggest that the control effectiveness for small deflections for these unswept configurations of conventional thickness would probably reverse at Mach numbers in the neighborhood of 0.9.

Further light is shed on this phenomenon by results obtained from wing-flow tests (references 11 and 12), which are shown in figure 11. This plot shows the control-effectiveness parameter C_{L_δ}, measured over $\pm 4^\circ$ control deflection, plotted against Mach number. Data are shown for an unswept configuration of 10-percent thickness, the actual sweep of leading edge being 13°, and for a 35° sweptback configuration of 9-percent thickness. It is noted that the control effectiveness for the unswept tail surface actually did reverse for small deflections at a Mach number of approximately 0.95. At higher Mach numbers the control regained effectiveness for small deflections. It may be noted also that the sweptback configuration did not lose completely its control effectiveness at any speed up to a Mach number of 1.10. Actually, the control effectiveness of the sweptback configuration fell off by about 40 percent from its low-speed value. Although these data were obtained at very low Reynolds number, that is, approximately one million, there is no proof that the phenomenon of control reversal shown by the unswept configuration will not occur also at higher Reynolds numbers, perhaps to a different degree. From figure 11 it should not be assumed that the unswept control had reversed effectiveness at all deflections.

Effect of deflection.- Figure 12 will show how the lift produced by the control varies with deflection at different Mach numbers for

the straight tail surface. One curve is for a Mach number of 0.85 where the force break occurred, one is for a Mach number of 0.96 where the control effectiveness was reversed, and one is for a Mach number of 1.04 where the control had regained effectiveness at all deflections.

It should be noted that, although the flap gave a net loss in lift between deflections of -4° and 4° at a Mach number of 0.96, as was shown in figure 11 by the negative value for C_{L_δ} at higher deflections, the flap produced lift in the proper direction. Hence, it would probably be possible to use such a control for trimming in combination with an adjustable stabilizer or an adjustable fin at transonic speeds, but it is believed everyone would object to such a control because of the illogical type of control motion it would introduce. In this connection, however, floating-model tests of very thin unswept airfoils have not shown reversed control effectiveness at transonic speeds for the moderately small deflections that were tested. Hence, it seems premature to condemn completely the use of unswept configurations at transonic speeds. Much more data is needed to determine the effects of airfoil thickness, of flap trailing-edge angle, and of possibly other geometric parameters on the flap effectiveness of unswept tail surfaces. For the present time, however, we know that the flap on the 9-percent-thick, 35° sweptback tail surface showed no signs of complete loss of effectiveness even for small deflection at any speed up to a Mach number of 1.10, the highest Mach number reached.

Design Procedure

Since the control lift effectiveness is so closely related to the aileron rolling effectiveness, the design of controls such as elevators on tailless aircraft will not be discussed in detail. The lift effectiveness parameter C_{L_δ} however showed about the same variation with sweep as did the aileron effectiveness; that is, there was a decrease in C_{L_δ} with increase in sweep and decrease in aspect ratio. (See fig. 13.) Reducing these data to eliminate the sweep angle and flap chord by dividing the values of C_{L_δ} at each spanwise station by $\cos^2\Lambda$ and α_δ of the "unswept" control gave an average curve except for the small-span controls on highly swept wings which again showed a loss in effectiveness. (See fig. 14.) The values of C_{L_δ} for other wings equipped with tip controls may be obtained in a manner similar to the aileron effectiveness, except that the aspect-ratio correction is the ratio of the lift-curve slope for the "unswept" wing to the lift-curve slope for aspect ratio 6 (K_3). (See fig. 14.) As with aileron effectiveness, the reliability of this method was checked by estimating C_{L_δ}

for nine wings and comparing with the measured value of C_{L_δ}. Good agreement was obtained for all wings except two for which the control was located other than at the tip. Since unswept lift data indicate the lift effectiveness is different for controls starting at the tip than for those starting at the root, this disagreement would probably be expected. Thus, in addition to the restriction placed on the method of prediction of aileron effectiveness, that is, aspect ratio and taper ratio, we must also limit this method to controls starting at the wing tip.

PITCH EFFECTIVENESS

Effects of Compressibility

In addition to a knowledge of the effects of compressibility on aileron characteristics and lift effectiveness, the designer of a high-speed flying-wing-type airplane needs to know what the effects of compressibility will be on the pitching moment produced by trailing-edge flaps. Here, the emphasis is on sweptback configurations almost entirely because of the necessity for providing a reasonably large, allowable, center-of-gravity range together with a reasonably high, trimmed, maximum lift coefficient. Some data showing the effects of compressibility on the pitching-moment effectiveness of longitudinal controls on sweptback wings are shown in figure 15.

This figure shows the pitching-moment parameter C_{m_δ} plotted against Mach number for various sweptback wing-flap combinations (reference 11). The pitching-moment slopes shown here are with reference to a point at 17 percent of the mean aerodynamic chord of each of the wings. This point was found to be the low-speed aerodynamic-center location for the isolated wings, having 35° and 45° of sweepback and an aspect ratio of 3, which are shown in this figure. It is seen that the effects of compressibility on pitching-moment control are relatively small at all speeds tested which are up to a Mach number of 1.1. The maximum loss in effectiveness of the $\frac{1}{4}$-chord plain flap on the 35° sweptback NACA 65-009 airfoil, which was the only configuration tested through the speed of sound, was about 30 percent. Partial-span flaps on the tapered 35° sweptback wing show a similar tendency to lose pitching-moment effectiveness as the speed of sound is approached. With 45° of sweepback, the longitudinal control effectiveness of the full-span 25-percent-chord flap on a 12-percent-thick wing was completely unaffected by compressibility up to a Mach number of 0.89. These data indicate that trailing-edge-type longitudinal controls will retain considerable pitching-moment effectiveness at transonic speeds if as much as 35° sweepback is used and if the wing thickness is not too great; for the cases under consideration the maximum thickness was about 12 percent.

Effects of Sweep

The limited amount of low-speed data for the effects of sweep and spanwise location on the pitch effectiveness does not permit the construction of design charts. The pitching-moment data for one series of swept wings do, however, show consistent variations with sweep for sweep angles greater than 30° (fig. 16) but are not complete enough to account for all the variables.

HINGE-MOMENT CHARACTERISTICS

Thus far only the effects of sweep and speed on the effectiveness of controls have been discussed. Unfortunately there are not sufficient high-speed data available as yet for developing reliable methods of predicting hinge-moment characteristics of control surfaces in the transonic speed range. Efforts to approach the problem theoretically have not yielded satisfactory results because of the lack of a suitable approach, which accounts for the many variables such as effects of the viscosity of the air, boundary layer, and separation. There is sufficient information, however, to show the variation of hinge moments with speed and sweep for several controls in the transonic speed range. The more significant data will be discussed first with respect to unbalanced control surfaces and then with respect to aerodynamically balanced surfaces.

Unbalanced Control Surfaces

Effects of sweep.- Sweep has been shown to be very useful in delaying the effects of compressibility on the effectiveness of control surfaces and in decreasing the magnitude of the changes when they occur. The same general trends exist in the hinge-moment characteristics.

In figure 17 are presented the variations of the aileron hinge-moment parameters C_{h_α} and C_{h_δ} with Mach number for three wings having varying degrees of sweep. (See reference 9.) The variations of hinge-moment coefficient with angle of attack and control-surface deflection are C_{h_α} and C_{h_δ}, respectively. It will be noted, as it was in the case with effectiveness, that the main effects of sweep of hinge moments are to delay the effects of compressibility to a higher Mach number and to decrease the magnitude of the changes when they occur. In the results shown here, C_{h_α} and C_{h_δ} are both negative, and the effect of sweep is to reduce the absolute value of the hinge-moment parameters with increasing sweep. In other tests in the Ames 16-foot high-speed tunnel of a model having a large trailing-edge angle, C_{h_α} and C_{h_δ} were positive for the unswept configurations, and sweeping the wing back tended to reduce the

positive values of the parameters. Thus, in these and other investigations, sweeping the model tended to reduce the magnitude of C_{h_α} and C_{h_δ}, whether the parameters were positive or negative for the unswept configuration. Such an effect is to be expected because the magnitudes of the hinge-moment parameters are directly related to the lift or loading parameter C_{L_δ}, which has been shown to decrease roughly as the cosine squared of the angle of sweep.

Trailing-edge angle.- The importance of control-surface profile aft of the hinge line on the high-speed control-surface characteristics has been fully realized only relatively recently (reference 26). In many high-speed wind-tunnel and flight investigations, drastic changes in control-surface characteristics were unexpectedly encountered at high Mach numbers. In some cases, the unusual characteristics were found to be associated with bulges and in others with the trailing-edge angle of the control surface. Analysis of the results indicated that adverse effects generally came with the larger trailing-edge angle, which for bulged and cusped surfaces are best measured between the maximum tangents to the surface. The larger the trailing-edge angle, the more positive became C_{h_α} and C_{h_δ} and the greater the increase of these parameters with increasing Mach number. This trend occurs for both unswept and swept control-surface combinations.

In figure 18 are presented the variations of C_{h_α} and C_{h_δ} with Mach number for three swept models having different trailing-edge angles. The trailing-edge angles indicated in the figure are those measured parallel to the wind stream. It can be seen that increasing the trailing-edge angle increases C_{h_α} and C_{h_δ} and leads to adverse changes with increasing Mach number. The large positive C_{h_δ} above 0.6 Mach number of the control surface having the greatest trailing-edge angle did not extend over the entire control-surface-deflection range but did cover the useful operating range as shown in figure 19. (See reference 14.) Although the aileron had a radius nose, considerable balancing effect was produced by the large trailing-edge angle at all Mach numbers, the degree of balance increasing rapidly at the higher Mach numbers, the ailerons then becoming overbalanced. At the same time the control effectiveness changed in a similar manner, reversed effectiveness occurring in the same general range as the positive C_{h_δ}. The airfoil section perpendicular to the quarter-chord line was the NACA 0011-64 section. Extension of the chord and reduction of the trailing-edge angle as indicated in figure 19 materially improved the hinge-moment characteristics as well as causing a similar improvement in the effectiveness of the control surface and in the stability characteristics of the wing.

These results indicate that the trailing-edge angle should be kept to a minimum, preferably below 14°. In doing so, flat-sided control surfaces may be generally preferable to cusped surfaces both from a structural standpoint and because a cusp tends to heavy the hinge moments

by negatively increasing C_{h_δ}. Bulges and bevels are definitely not suitable for high-speed use because of the accompanying large trailing-edge angles. Special care should be taken when using elliptical plan forms or curved trailing edges in order that the trailing-edge angles be kept uniformly small along the entire span of the control surface.

Aerodynamically Balanced Control Surfaces

Overhang.- Aerodynamic balancing of control surfaces is often desirable even where boosts are employed in the system (reference 26). The most common type of balance is the nose overhang, shown on three models in figure 20. The variations of C_{h_α} and C_{h_δ} with Mach number are presented for each of the three models, all of which had trailing-edge angles of 14° or less. Only the first model displayed an objectionable increase in C_{h_α} and C_{h_δ} with increasing Mach number over the test range. This was caused by the larger thickness of the overhang forward of the hinge line. These results and other similar data indicate that overhang balances can be used up to a Mach number of at least 0.85 and probably higher, provided the nose shape is properly formed and the thickness-to-chord ratio and trailing-edge angles are kept small. There is very little data on internal nose balances above 0.8 Mach number, but the same general remarks apply.

Tabs.- In figure 21 is shown the effect of sweep on tab effectiveness. Existing data on tabs indicate that the tab effectiveness generally decreases at high Mach numbers in a manner similar to that of the flap-effectiveness parameter C_{L_δ}, since the same factors, such as separation, influence both. The results show that sweeping the hinge line back 45° reduced the tab effectiveness at lower Mach numbers as might be expected but also resulted in a more faborable variation with Mach number. These effects of sweep on tab effectiveness are very similar to the effects of sweep on C_{L_δ}, which have already been discussed.

Horn balance.- In figure 22 is shown a collection of hinge-moment data (reference 11 and unpublished data) for horn balances on swept tail surfaces. Results are shown for a 35° sweptback model with and without the horn obtained from wing-flow tests and for a 45° swept model with a horn from wind-tunnel tests. It can be seen that the values of C_{h_δ} for the 35° and 45° swept tails having horn balances are very nearly constant with Mach number below a Mach number of 0.9. At the low Reynolds number of about 0.8×10^6, the horn on the 35° swept model loses effectiveness rather rapidly above a Mach number of 0.9; but at a higher Reynolds number, the effectiveness appears to hold at least to the speed of sound. The results for the horn on the 45° swept model at the left of figure 6, which was at a Reynolds number of about 6×10^6, shows the same trend as the high Reynolds number data on the 35° swept wings. The large Reynolds number effects, such as shown here, make it difficult to predict the characteristics at full-scale Reynolds number from tests of relatively

small models because of the large influence of separation and boundary layer on trailing-edge type of controls.

The values of C_{h_α} for the horn balance on both the 35° and 45° swept tails are positive. It should be noted, however, that the unbalanced flap on the 35° swept wing gave almost zero C_{h_α} and most types of aerodynamic balance, with some exceptions, would be expected to give some positive increments of C_{h_α}.

The data presented indicate that the horn-type of balance apparently balances C_{h_δ} through Mach numbers of 1 but that the increasingly positive values of C_{h_α} with increasing Mach number might prohibit its use except for truly irreversible control systems where, for example, oscillations such as snaking offer no problem. In any case, the balancing power of the horn would be reduced by the positive C_{h_α}, which tends to heavy the controls during maneuvers because the combination of C_{h_α} and C_{h_δ} determined the resulting hinge moments and control forces in flight.

CONCLUSIONS

It appears from the data presented that no serious problems resulting from compressibility effects will be encountered so long as the speeds are kept below the critical speed of the wing or tail surface and the trailing-edge angle is kept small, that is, less than about 14°. Above critical speeds, however, the behavior of the control depends to a large extent on the wing sweep angle. The main effects of sweeping the wing or tail are to postpone to higher Mach numbers the adverse effects of compressibility and to decrease these adverse effects when they occur. The design procedures presented, although of a preliminary nature, appear to offer a method of estimating the effectiveness of flap-type controls on swept wings of normal aspect ratio and taper ratio.

Langley Memorial Aeronautical Laboratory
National Advisory Committee for Aeronautics
Langley Field, Va.

REFERENCES

1. Langley Research Department: Summary of Lateral-Control Research (Compiled by Thomas A. Toll.) NACA TN No. 1245, 1947.

2. Weick, Fred E., and Jones, Robert T.: Résumé and Analysis of N.A.C.A. Lateral Control Research. NACA Rep. No. 605, 1937.

3. Ames, Milton B., Jr., and Sears, Richard I.: Determination of Control-Surface Characteristics from NACA Plain-Flap and Tab Data. NACA Rep. No. 721, 1941.

4. Crane, Robert M.: Computation of Hinge-Moment Characteristics of Horizontal Tails from Section Data. NACA CB No. 5B05, 1945

5. Swanson, Robert S., and Crandall, Stewart M.: Lifting-Surface-Theory Aspect-Ratio Corrections to the Lift and Hinge-Moment Parameters for Full-Span Elevators on Horizontal Tail Surfaces. NACA TN No. 1175, 1947.

6. Fischel, Jack, and Ivey, Margaret F.: Collection of Test Data for Lateral Control with Full-Span Flaps. NACA TN No. 1404, 1947.

7. Pitkin, Marvin, and Maggin, Bernard: Analysis of Factors Affecting Net Lift Increment Attainable with Trailing-Edge Split Flaps on Tailless Airplanes. NACA ARR No. L4I18, 1944.

8. Luoma, Arvo A.: An Investigation of a High-Aspect-Ratio Wing Having 0.20-Chord Plain Ailerons in the Langley 8-Foot High-Speed Tunnel. NACA RM No. L6H28d, 1946.

9. Luoma, Arvo A., Bielat, Ralph P., and Whitcomb, Richard T.: High-Speed Wind-Tunnel Investigation of the Lateral-Control Characteristics of Plain Ailerons on a Wing with Various Amounts of Sweep. NACA RM No. L7I15, 1947.

10. Sandahl, Carl A., and Strass, H. Kurt: Additional Results in a Free-Flight Investigation of Control Effectiveness of Full-Span, 0.2-Chord Plain Ailerons at High Subsonic, Transonic, and Supersonic Speeds to Determine Some Effects of Wing Sweepback, Aspect Ratio, Taper, and Section Thickness Ratio. NACA RM No. L7L01, 1947.

11. Johnson, Harold I.: Measurements of the Aerodynamic Characteristics of a 35° Sweptback NACA 65-009 Airfoil Model with $\frac{1}{4}$-Chord Plain Flap by the NACA Wing-Flow Method. NACA RM No. L7F13, 1947.

12. Adams, Richard E., and Silsby, Norman S.: Tests of a Horizontal-Tail Model through the Transonic Speed Range by the NACA Wing-Flow Method. NACA RM No. L7C25a, 1947.

13. Bielat, Ralph P.: Investigation at High Speeds of a Horizontal-Tail Model in the Langley 8-Foot High-Speed Tunnel. NACA RM No. L6L10b, 1947.

14. Boddy, Lee E., and Morrill, Charles P., Jr.: The Aerodynamic Effects of Modifications to the Wing and Wing-Fuselage Intersection of an Airplane Model with the Wing Swept Back 35°. NACA RM No. A7J02, 1947.

15. Schuldenfrei, Marvin, Comisarow, Paul, and Goodson, Kenneth W.: Stability and Control Characteristics of an Airplane Model Having a 45.1° Swept-Back Wing with Aspect Ratio 2.50 and Taper Ratio 0.42 and 42.8° Swept-Back Horizontal Tail with Aspect Ratio 3.87 and Taper Ratio 0.49. NACA RM No. L7B25, 1947.

16. Goodson, Kenneth W., and Comisarow, Paul: Lateral Stability and Control Characteristics of an Airplane Model Having a 42.8° Swept-back Circular-Arc Wing with Aspect Ratio 4.00, Taper Ratio 0.50, and Sweptback Tail Surfaces. NACA RM No. L7G31, 1947.

17. Gilruth, R. R., and Wetmore, J. W.: Preliminary Tests of Several Airfoil Models in the Transonic Speed Range. NACA ACR No. L5E08, 1945.

18. Daum, Fred L., and Sawyer, Richard H.: Tests at Transonic Speeds of the Effectiveness of a Swept-Back Trailing-Edge Flap on an Airfoil Having Parallel Flat Surfaces, Extreme Sweepback, and Low Aspect Ratio. NACA CB No. L5H01, 1945.

19. Bennett, Charles V., and Johnson, Joseph L.: Experimental Determination of the Damping in Roll and Aileron Rolling Effectiveness of Three Wings Having 2°, 42°, and 62° Sweepback. NACA TN No. 1278, 1947.

20. Letko, William, and Goodman, Alex: Preliminary Wind-Tunnel Investigation at Low Speed of Stability and Control Characteristics of Swept-Back Wings. NACA TN No. 1046, 1946.

21. Feigenbaum, David, and Goodman, Alex: Preliminary Investigation at Low Speeds of Swept Wings in Rolling Flow. NACA RM No. L7E09, 1947.

22. Schueller, Carl F., Korycinski, Peter F., and Strass, H. Kurt: Tests of a Full-Scale Horizontal Tail Surface in the Langley 16-Foot High-Speed Tunnel. NACA TN No. 1074, 1946.

23. Schueller, Carl F., Hieser, Gerald, and Cooper, Morton: Aerodynamic Force Characteristics at High Speeds of a Full-Scale Horizontal Tail Surface Tested in the Langley 16-Foot High-Speed Tunnel. NACA RM No. L7D08a, 1947.

24. Lindsey, W. F.: Effect of Compressibility on the Pressures and Forces Acting on a Modified NACA 65,3-019 Airfoil Having a 0.20-Chord Flap. NACA ACR No. L5G31a, 1946.

25. Ilk, Richard J.: Characteristics of a 15-Percent-Chord and a 35-Percent-Chord Plain Flap on the NACA 0006 Airfoil Section at High Subsonic Speeds. NACA RM No. A7H19, 1947.

26. Axelson, John A.: A Summary and Analysis of Wind-Tunnel Data on the Lift and Hinge-Moment Characteristics of Control Surfaces up to a Mach Number of 0.90. NACA RM No. A7L02, 1947.

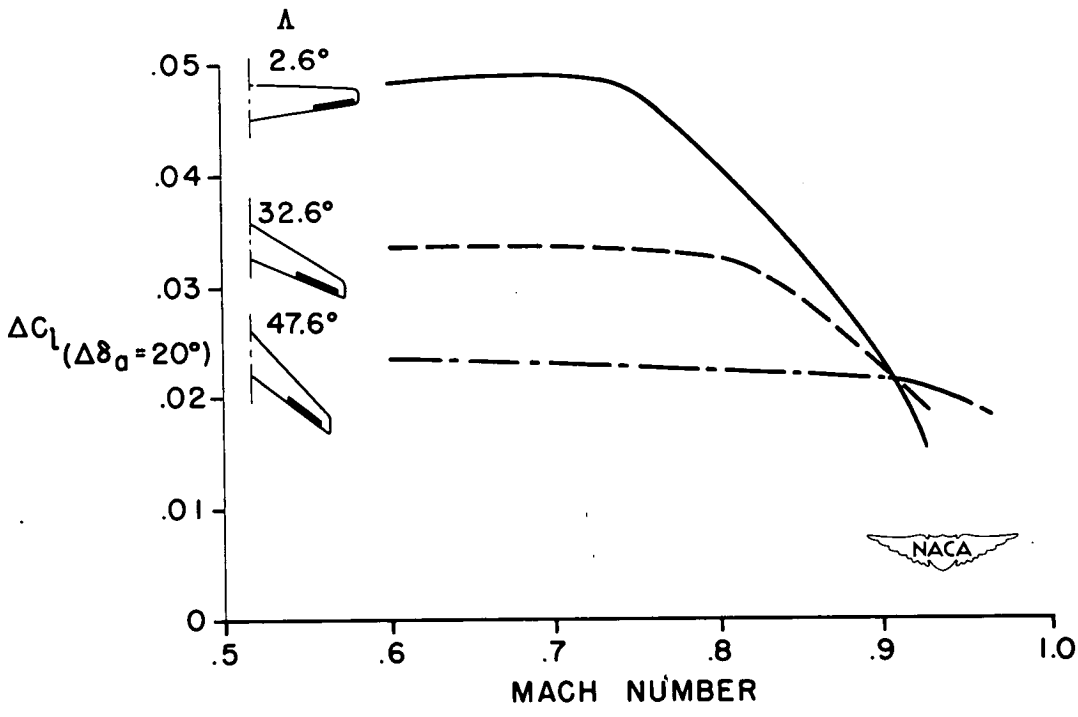

AILERON EFFECTIVENESS AT HIGH SUBSONIC SPEEDS

Figure 1.

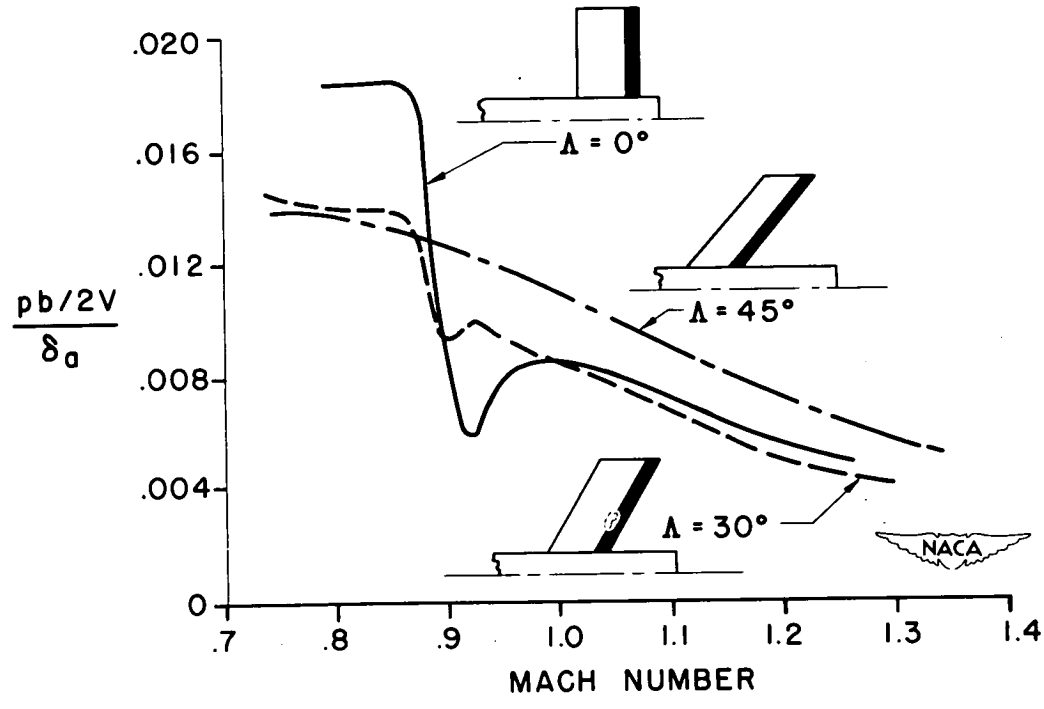

ROLLING EFFECTIVENESS AT TRANSONIC SPEEDS

Figure 2.

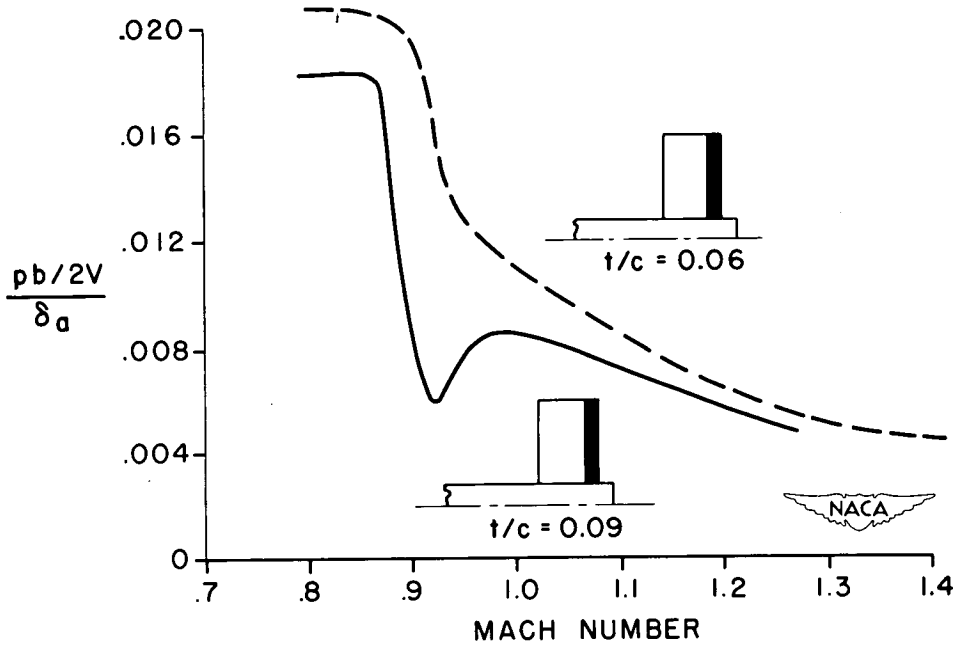

EFFECT OF THICKNESS ON ROLLING EFFECTIVENESS AT TRANSONIC SPEEDS

Figure 3.

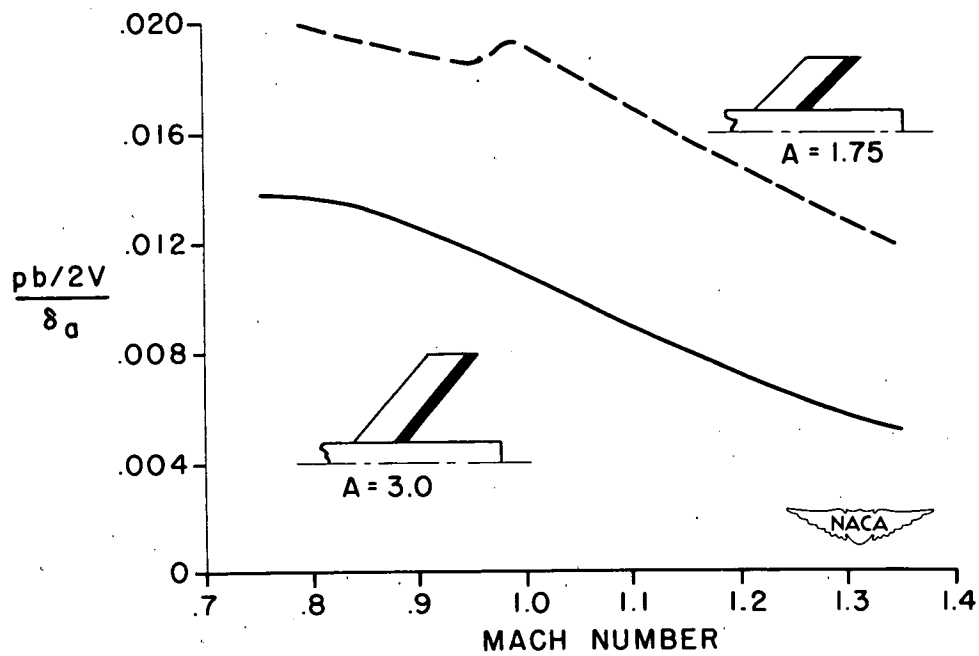

EFFECT OF ASPECT RATIO ON ROLLING EFFECTIVENESS AT TRANSONIC SPEEDS

Figure 4.

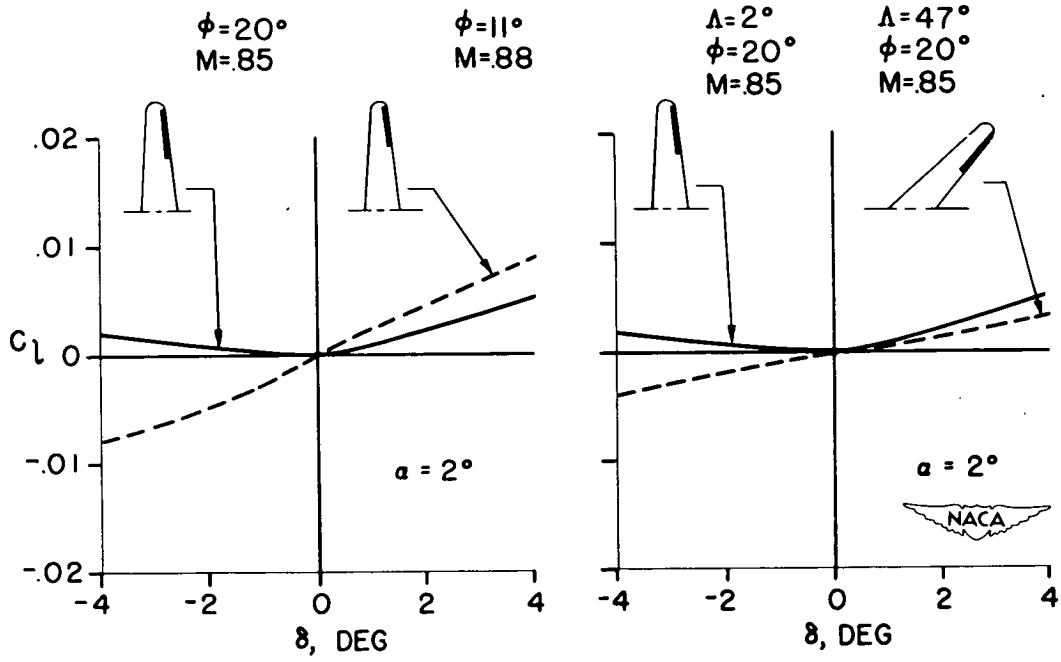

EFFECTS OF TRAILING-EDGE ANGLE AND SWEEP ON AILERON EFFECTIVENESS

Figure 5.

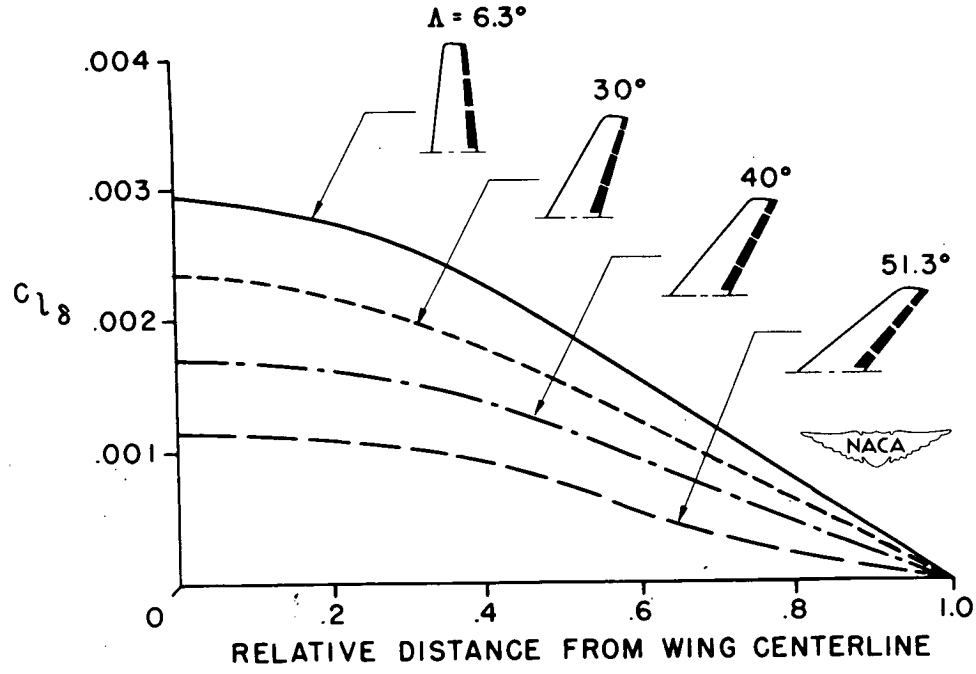

EFFECT OF SWEEP AND SPANWISE LOCATION ON AILERON EFFECTIVENESS

Figure 6.

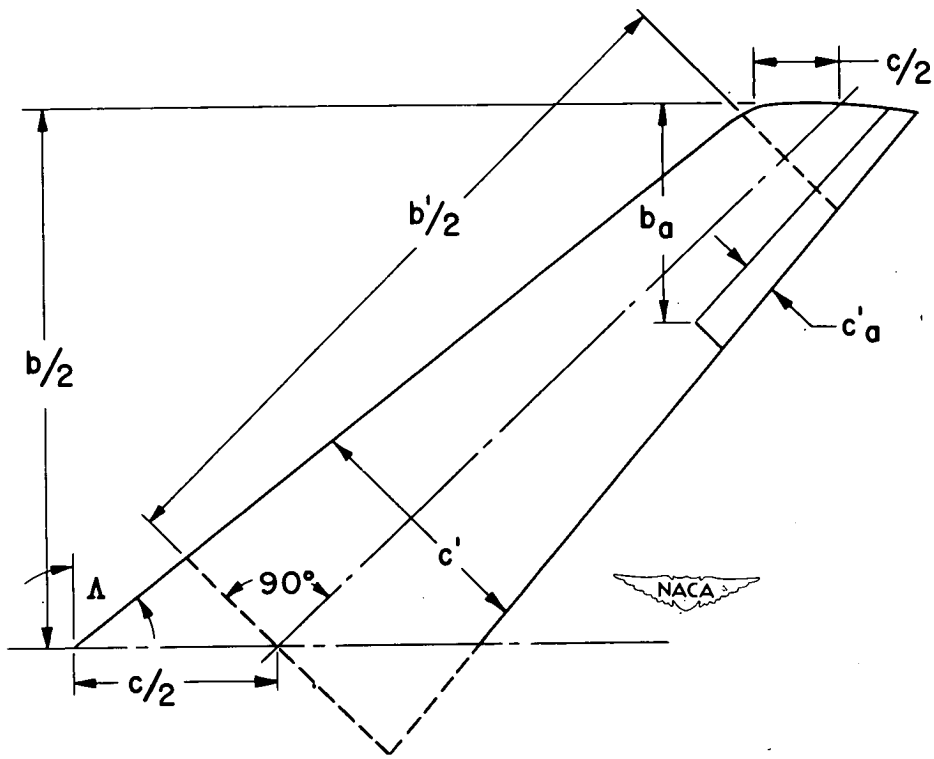

Swept-wing nomenclature.

Figure 7.

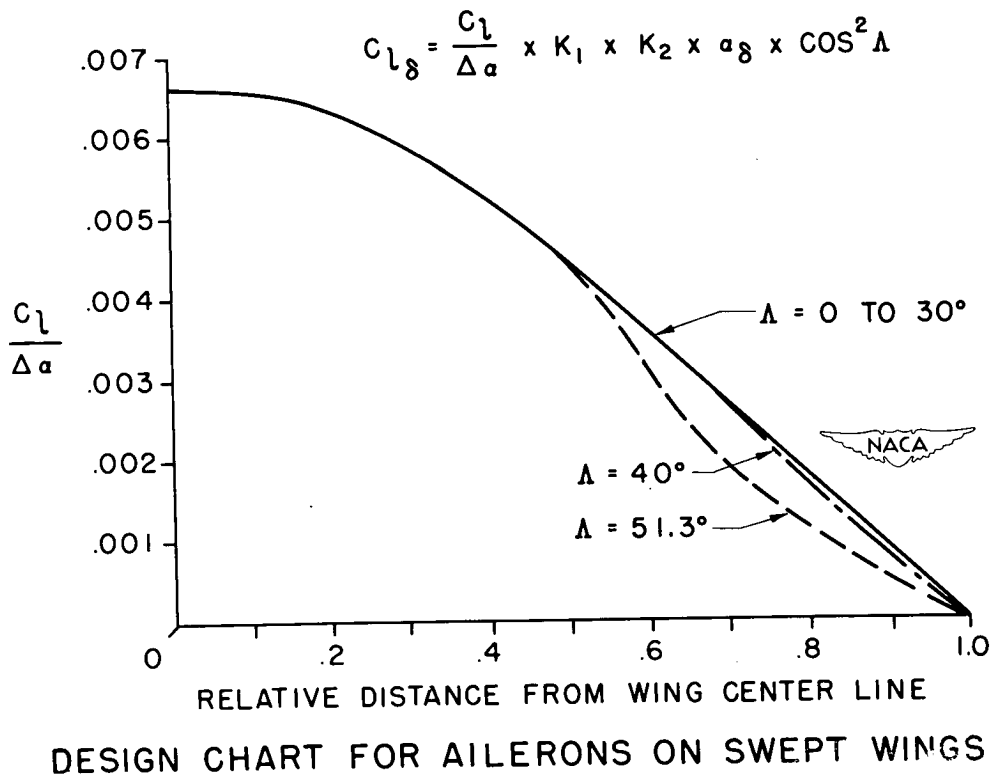

Figure 8.

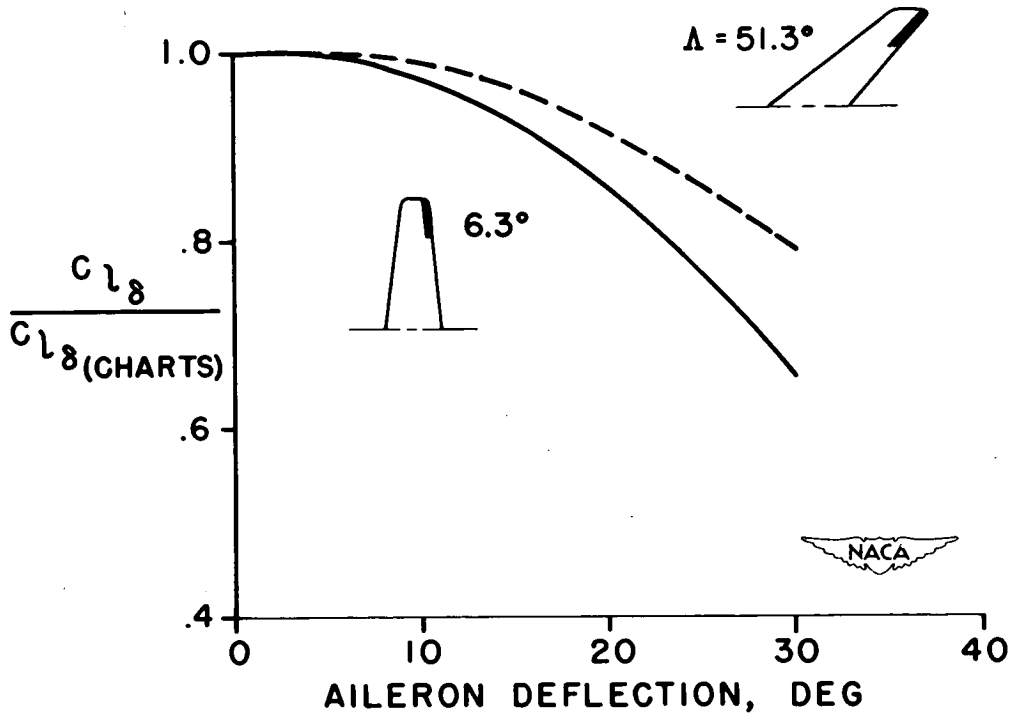

LOSS IN EFFECTIVENESS AT LARGE DEFLECTIONS

Figure 9.

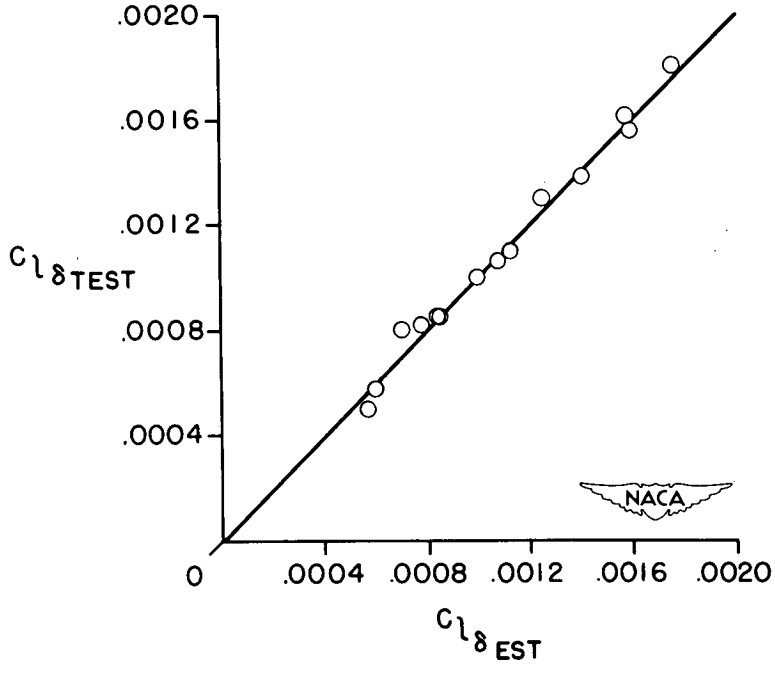

COMPARISON OF ESTIMATED AND EXPERIMENTAL AILERON EFFECTIVENESS

Figure 10.

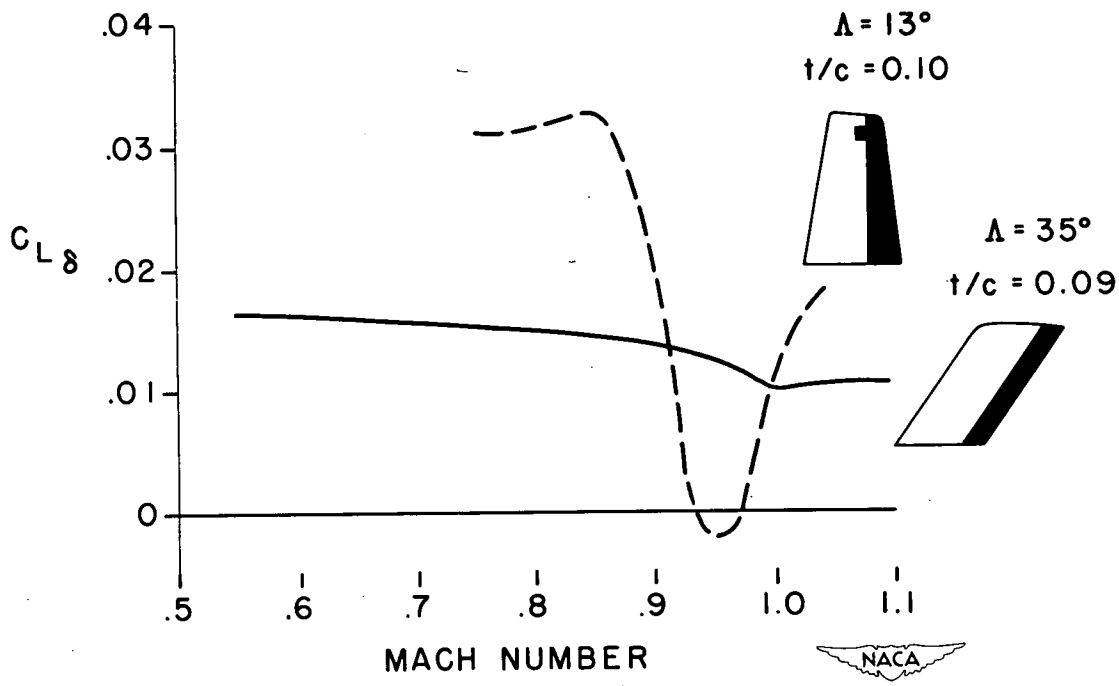

CONTROL EFFECTIVENESS AT TRANSONIC SPEEDS

Figure 11.

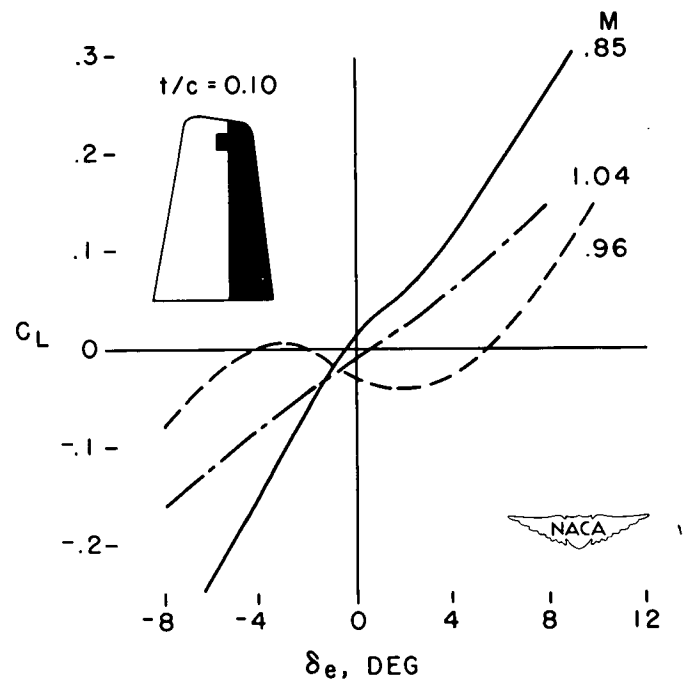

VARIATION OF CONTROL EFFECTIVENESS WITH DEFLECTION

Figure 12.

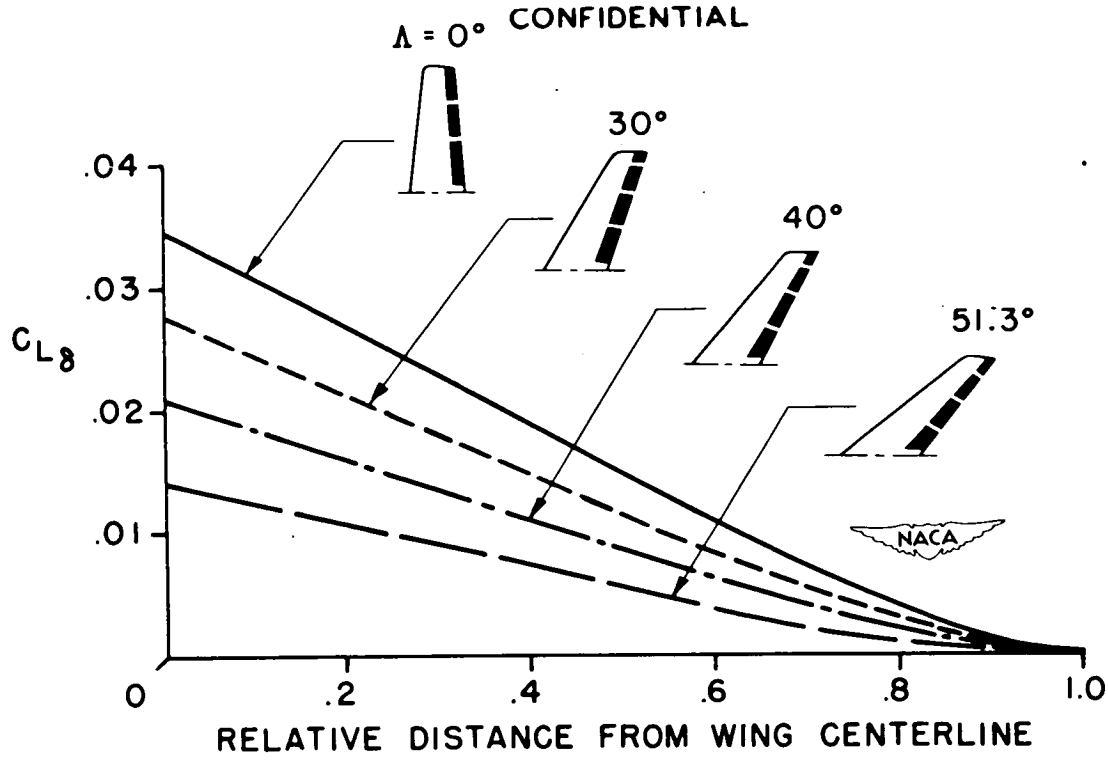

Effect of sweep and spanwise location on control effectiveness.

Figure 13.

$$C_{L_\delta} = \frac{C_{L_\delta}}{a_\delta} \times K_3 \times a_\delta \times \cos \Lambda^2$$

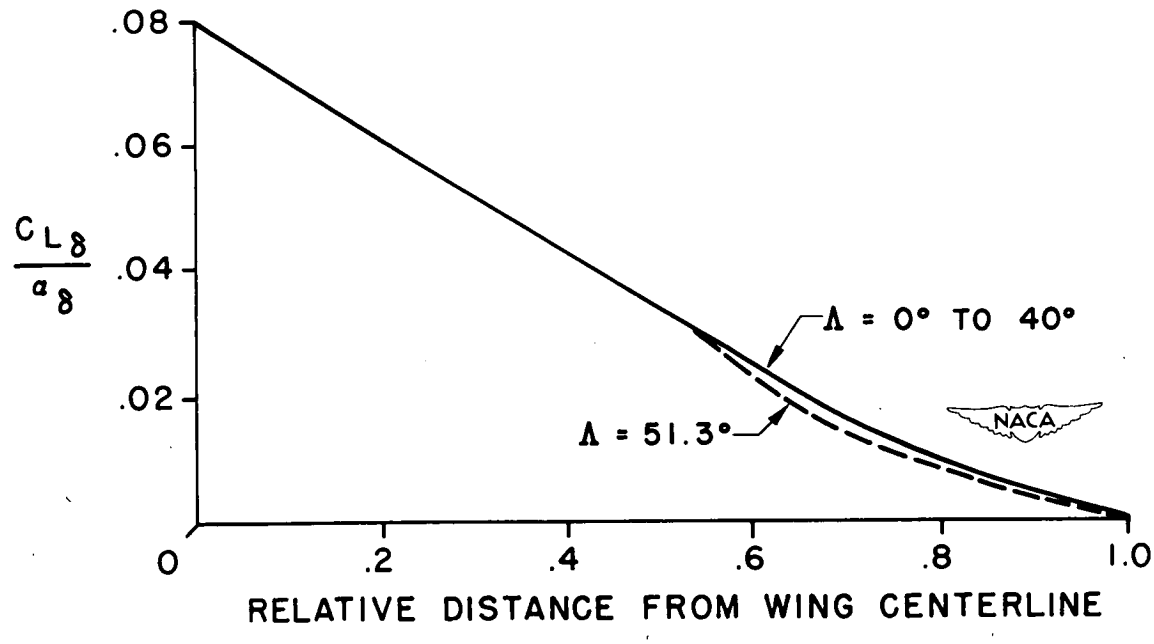

Design chart for C_{L_δ} on swept wing.

Figure 14.

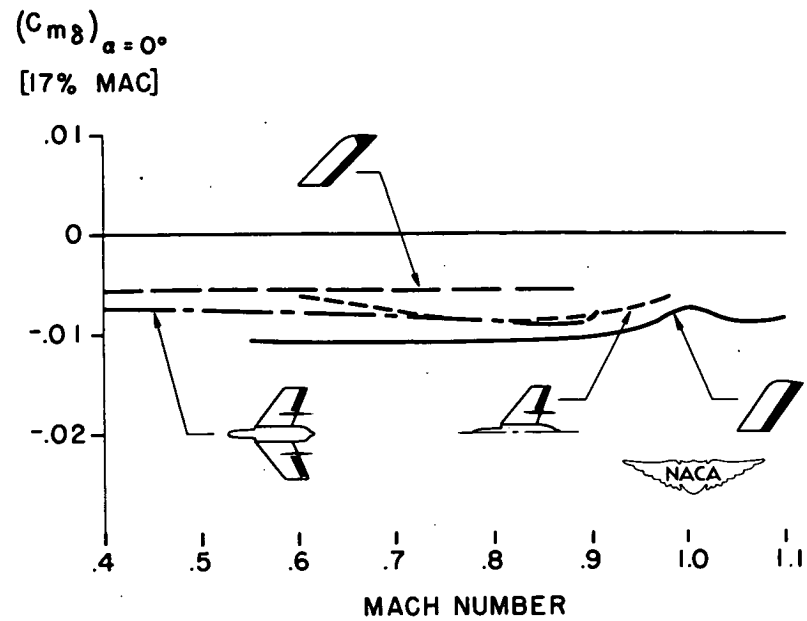

PITCH CONTROL AT TRANSONIC SPEEDS

Figure 15.

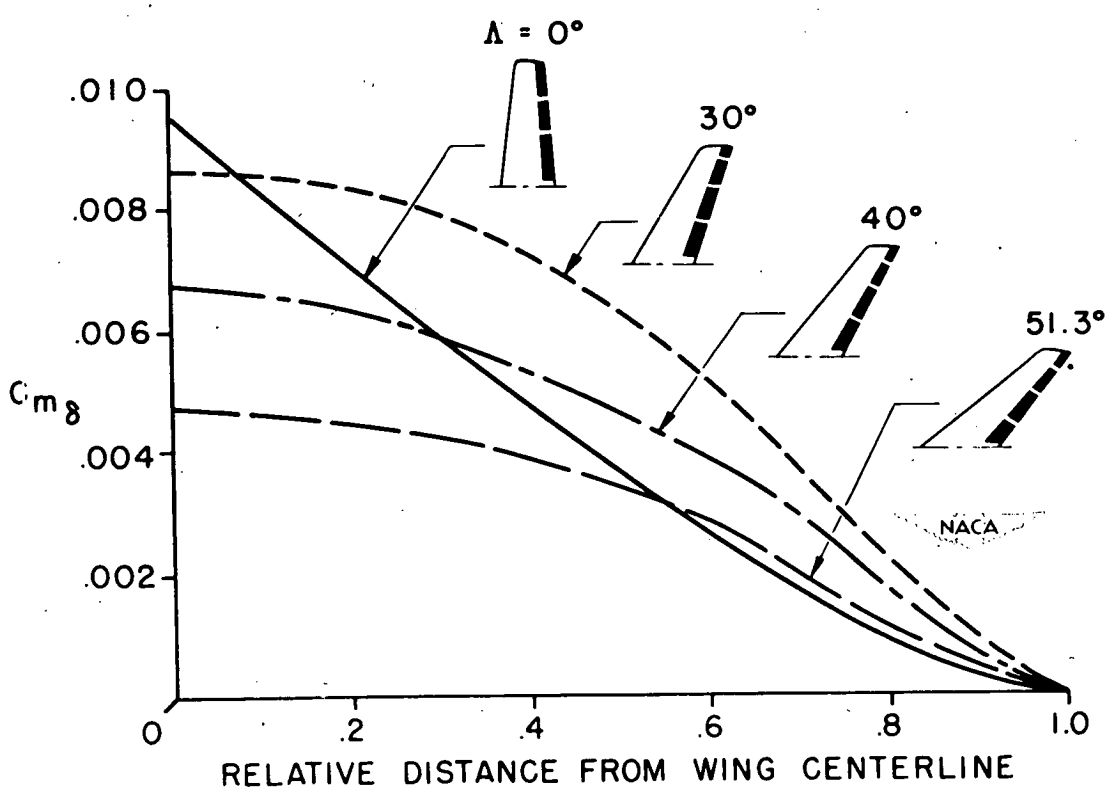

Effect of sweep and span on C_{m_δ}.

Figure 16.

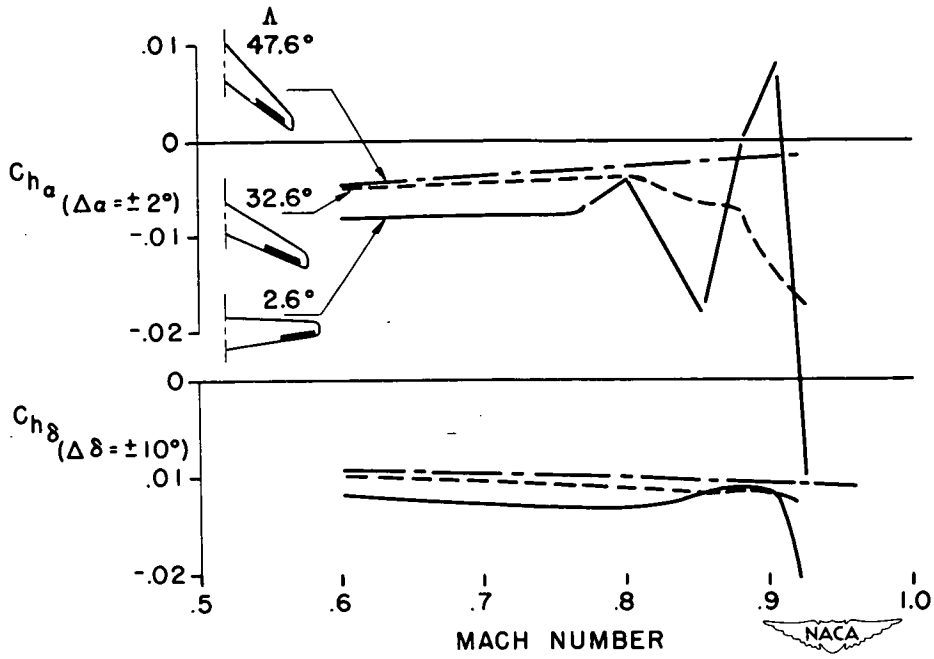

AILERON HINGE-MOMENT PARAMETERS AT HIGH SUBSONIC SPEEDS

Figure 17.

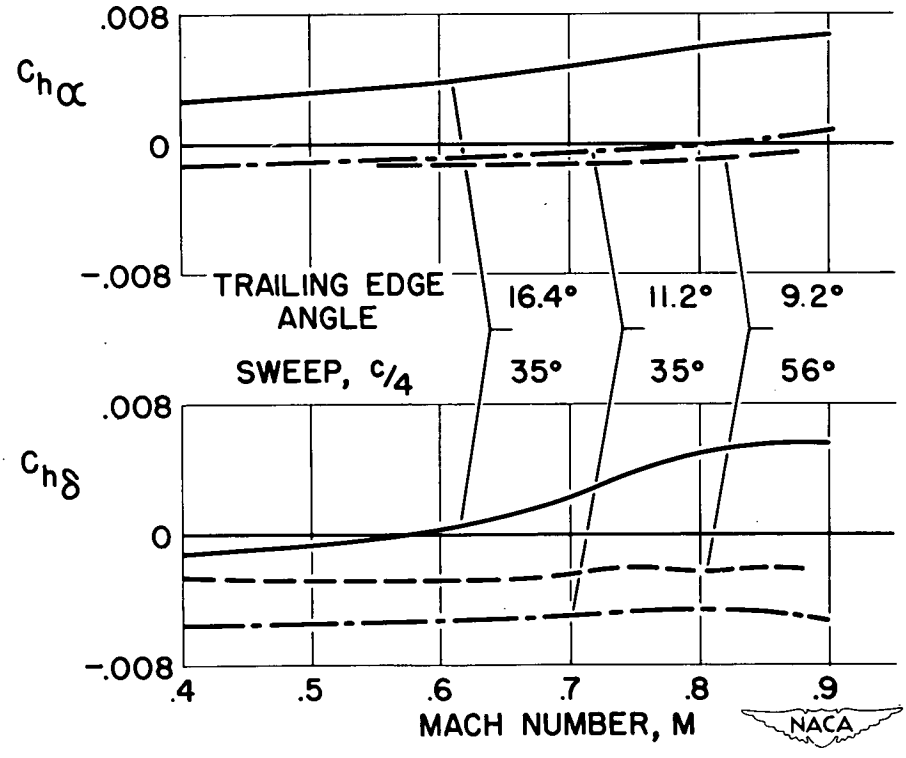

Effect of Trailing-Edge Angle on Hinge-Moment Parameters.

Figure 18.

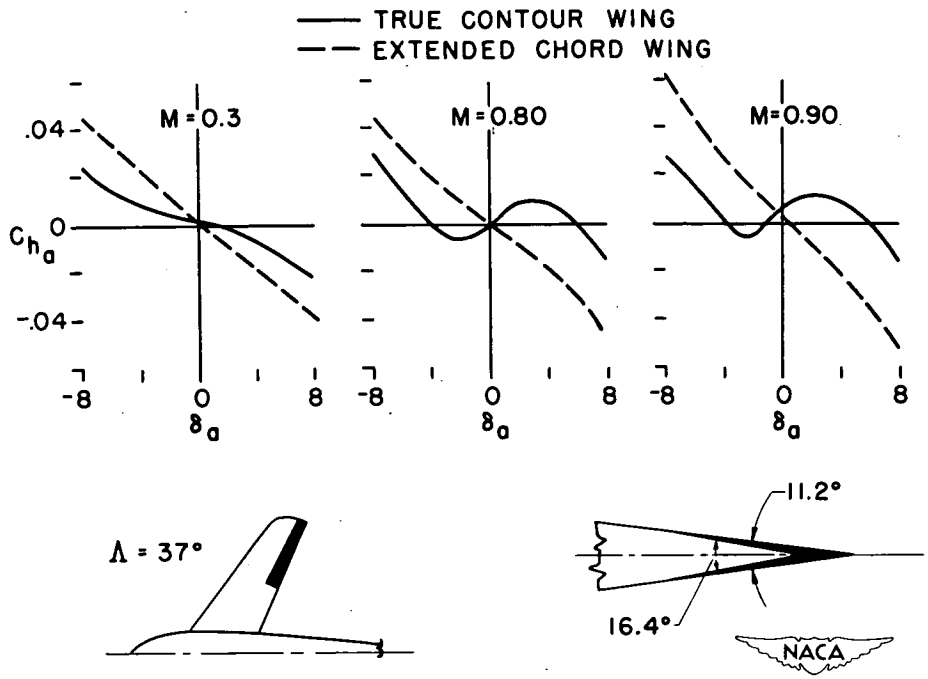

EFFECT OF TRAILING-EDGE ANGLE AT HIGH SUBSONIC SPEEDS

Figure 19.

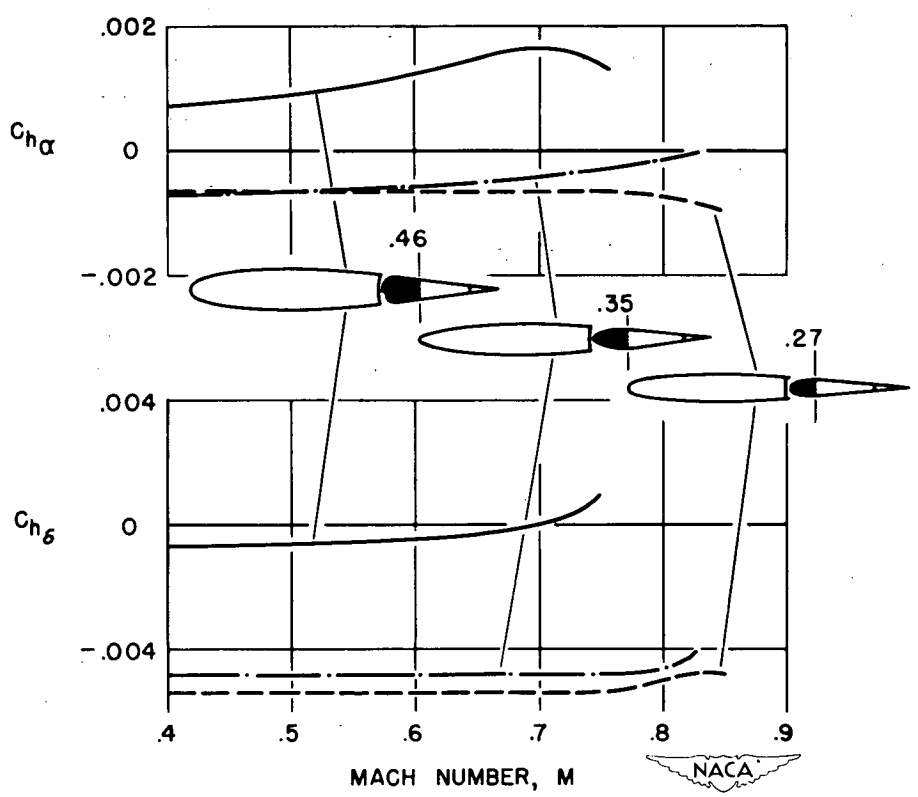

Effect of Nose Balance on Hinge-Moment Parameters.

Figure 20.

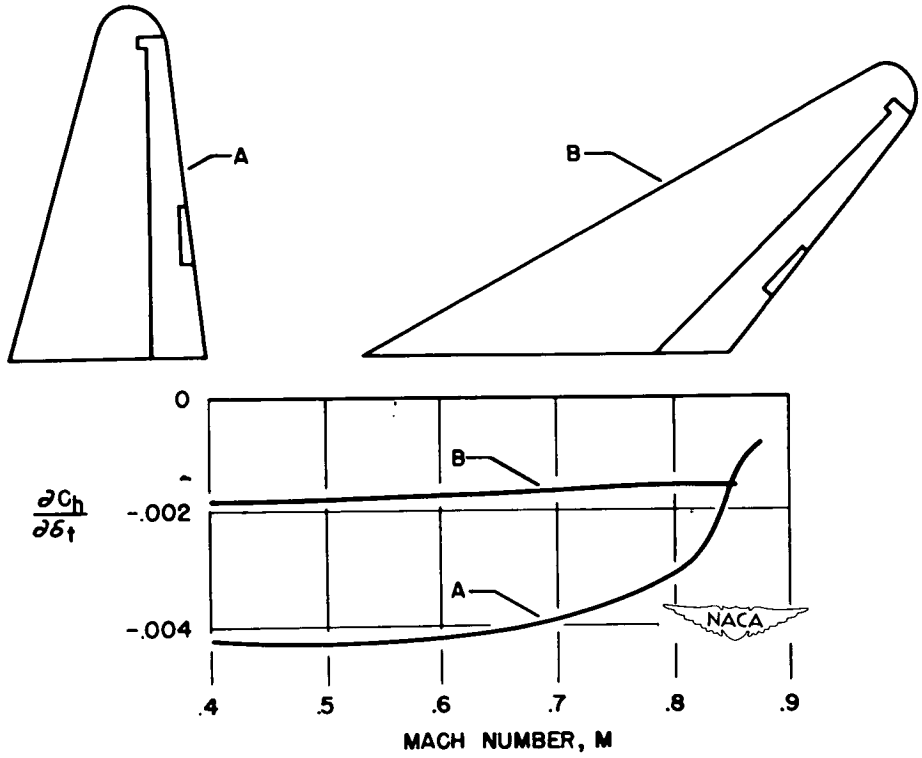

Effect of Sweep on Tab Effectiveness.

Figure 21.

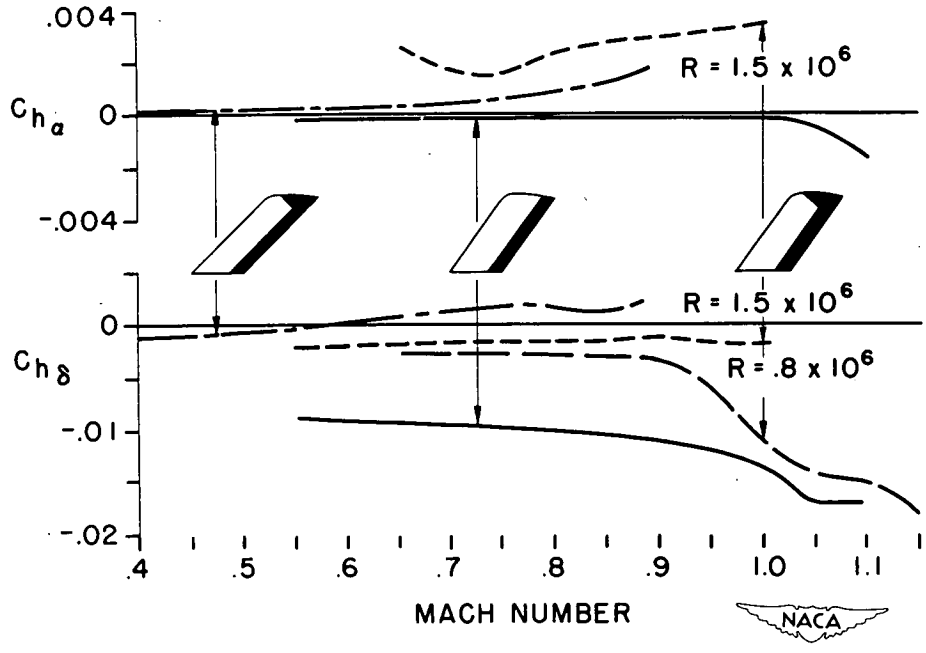

HINGE-MOMENT PARAMETERS AT TRANSONIC SPEEDS

Figure 22.